A Hypothetical Dense 3,4-Connected Carbon Net and Related B₂C and CN₂ Nets Built from 1,4-Cyclohexadienoid Units

Michael J. Bucknum and Roald Hoffmann*

*Contribution from the Department of Chemistry, Cornell University,
Ithaca, New York 14853-1301*

Received June 17, 1994⊗

Abstract: This paper describes the geometrical and electronic structure of a hypothetical 3,4-connected tetragonal allotrope of carbon (space group $P4_2/mmc$, No. 131) built from 1,4-cyclohexadiene rings. The three-dimensional net, containing trigonal and tetrahedral atoms in a ratio of 2:1, has a calculated density of 3.12 g/cm³, intermediate between graphite and diamond. Band structure calculations for this net have been performed using the extended Hückel method. One-dimensional substructures of a polyquinoid, polyspiroquinoid, and polycyclophane nature are instructive in approaching the electronic structure of the full net. These substructures point to the importance of through-space interactions of the stacked olefin units in the net, separated by only 2.53 Å. It is apparent that interaction leads to substantial dispersion of the π and π^* bands, the highest occupied and lowest unoccupied bands in the tetragonal structure, respectively. The resulting density of states profile is that of a metal, with a significant $\pi-\pi^*$ band overlap at the Fermi level. Related nets formed by substituting boron and nitrogen into the trigonal sites of the lattice are studied as well. The electron count on the atom in the trigonal sites in the lattice significantly affects the band structure about the Fermi level; B₂C should be metallic, and CN₂ an insulator.

Diamond, graphite, and C₆₀[1] are allotropes of carbon in which space is filled with perfectly tetrahedral, perfectly trigonal, and approximately trigonal carbon atoms, respectively. These structures are not the only ones to fill space in this way,[2] at least on paper.[3] Of special interest are possible allotropes which would be dense, have interesting properties (e.g. conductivity), and share some of the structural features of the known allotropes, their 3- and 4-connectedness[4] for instance.

In this contribution we suggest one hypothetical carbon structure which combines 3- and 4-connected atoms, built upon the 1,4-cyclohexadiene motif,[5] **1**, and look at its likely electronic

properties. The space-filling structure in question is shown in
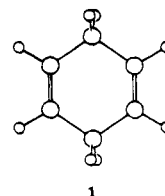
1

2. The net has tetragonal (space group $P4_2/mmc$, No. 131)

---

(1) (a) Wells, A. F. *Three Dimensional Nets and Polyhedra*; Wiley: New York, 1977. (b) Wells, A. F. *Further Studies of Three-Dimensional Nets*; ACA Monograph No. 8; American Crystallographic Association: Pittsburgh, 1979. (c) Donohue, J. *The Structure of the Elements*, Wiley: New York, 1974. (d) Krätschmer, W.; Huffmann, H. *Nature* **1990,** *347,* 354. (e) Kroto, H.; Heath, J. R.; O'Brien, S. C.; Curl, R. F.; Smalley, R. F. *Nature* **1985,** *318,* 162. (f) Osawa, E. *Kagaku* **1970,** *25,* 85. (g) Bundy, F. P.; Kasper, J. S. *J. Chem. Phys.* **1967,** *46,* 3437. (h) Aust, R. B.; Drickamer, H. G. *Science* **1963,** *140,* 817.

(2) (a) Zeger, L.; Kaxiras, E. *Phys. Rev. Lett.* **1993,** *70,* 2920—2922. (b) Muller, D. A.; Tzou, Y.; Raj, R.; Silcox, J. *Nature* **1993,** *366,* 725. (c) Renschler, C. L.; Pouch, J.; Cox, D. M. Eds. *Novel Forms of Carbon*; Materials Research Society Symposium Proceedings, Vol. 270; Materials Research Society: Pittsburgh, 1992. (d) Moshary, F.; Chen, N. H.; Silvera, I. F.; Brown, C. A.; Dorn, H. C.; de Vries, M. S.; Bethune, D. S. *Phys. Rev. Lett.* **1992,** *69,* 466—469. (e) Iijima, S. *Nature* **1991,** *354,* 56. (f) Utsumi, W.; Yagi, T. *Science* **1991,** *252,* 1542—1544. (g) Hirai, H.; Kondo, K. *Science* **1991,** *253,* 772—774. (h) Spear, K. E.; Phelps, A. W.; White, W. B. *J. Mater. Res.* **1990,** *5,* 2277. (i) Angus, J. C.; Hayman, C. C. *Science* **1988,** *241,* 1988. (j) Stankevich, V.; Nikerov, M. V.; Bochvar, D. A. *Russ. Chem. Rev.* **1987,** *53,* 670. (k) Melnitchenko, V. M.; Nikulin, Y. N.; Sladkov, A. M. *Carbon* **1985,** *23,* 3—7. (l) Stankevich, I. V.; Nikerov, M. V.; Bochvar, D. A. *Russ. Chem. Rev.* **1984,** *53,* 640. (m) Whittaker, A. G.; Watts, E. J.; Lewis, R. S.; Anders, E. *Science* **1980,** *209,* 1512—1514. (n) Whittaker, A. G.; Tooper, B. *J. Am. Ceram. Soc.* **1974,** *57,* 443—446. (o) Bochvar, D. A.; Galpern, E. G. *Dokl. Akad. Nauk. SSSR* **1973,** *209,* 612. (p) El Gorsey, A.; Donnay, G. *Science* **1968,** *161,* 363—364. (q) Ergun, S. *Carbon* **1968,** *6,* 141—149. (r) Drickamer, H. *Science* **1967,** *156,* 1183—1188. (s) Bundy, F. P. *J. Chem. Phys.* **1963,** *38,* 631.

(3) (a) Baughman, R. H.; Galvao, D. S. *Chem. Phys. Lett.* **1993,** *211,* 110—118. (b) Baughman, R. H.; Galvao, D. S. *Nature* **1993,** *365,* 735—737. (c) Tanaka, K.; Okahara, K.; Okada, M.; Yamabe, T. *Chem. Phys. Lett.* **1992,** *191,* 469—472. (d) Karfunkel, H. R.; Dressler, R. *J. Am. Chem. Soc.* **1992,** *114,* 2285—2288. (e) Diederich, F.; Rubin, Y. *Angew Chem., Int. Ed. Engl.* **1992,** *31,* 1101—1123. (f) Boercker, D. *Phys. Rev. B* **1991,** *44,* 11592. (g) Liu, A. Y.; Cohen, M. L.; Hass, K. C.; Tamon, M. A. *Phys. Rev. B* **1991,** *43,* 6742. (h) Mailhot, C.; McMahan, A. K. *Phys. Rev. B* **1991,** *44,* 11578. (i) Laqua, G.; Musso, H.; Boland, W.; Ahlrichs, R. *J. Am. Chem. Soc.* **1990,** *112,* 7391. (j) Tamor, M. A.; Hass, K. C. *J. Mater. Res.* **1990,** *5,* 2273. (k) Johnston, R. L.; Hoffmann, R. *J. Am. Chem. Soc.* **1989,** *111,* 810. (l) Baughman, R. H.; Eckhardt, H.; Kertesz, M. *J. Chem. Phys.* **1987,** *87,* 6687—6699. (m) Robertson, J.; O'Reilly, E. P. *Phys. Rev. B* **1987,** *35,* 2946. (n) Balaban, A. T. *Comput. Math. Appl.* **1987,** *17,* 397. (o) Stein, S. E.; Brown, R. L. *J. Am. Chem. Soc.* **1987,** *109,* 3721. (p) Burdett, J. K.; Lee, S. *J. Am. Chem. Soc.* **1985,** *107,* 3050, 3063, 3083. (q) Biswas, R.; Martin, R. M.; Needs, R. J.; Neilsen, O. H. *Phys. Rev. B* **1984,** *30,* 3210. (r) Hoffmann, R.; Hughbanks, T.; Kertesz, M.; Bird, P. H. *J. Am. Chem. Soc.* **1983,** *105,* 4831. (s) Kertesz, M.; Hoffmann, R. *J. Solid State Chem.* **1980,** *54,* 313. (t) Davidson, R. A. *Theor. Chim. Acta* **1981,** *58,* 193. (u) Hoffmann, R.; Eisenstein, O.; Balaban, A. T. *Proc. Natl. Acad. Sci. U.S.A.* **1980,** *77,* 5588. (v) Balaban, A. T.; Rentia, C. C.; Ciupitu, E. *Rev. Roum. Chim.* **1968,** *231,* 1233. (w) Pauling, L. *P.N.A.S.* **1966,** *56,* 1646. (x) Kakinoki, J. *Acta Crystallogr.* **1965,** *18,* 578. (y) Riley, H. L. *J. Chim. Phys.* **1950,** *47,* 565.

(4) Merz, K. M.; Hoffmann, R.; Balaban, A. T. *J. Am. Chem. Soc.* **1987,** *109,* 6742—6751.

(5) Balaban, A. T.; Klein, D. J.; Folden, C. A. *Chem. Phys. Lett.* **1994,** *217,* 266—270. This paper describes a series of related graphite-diamond hybrids, one of which is built from 1,4-cyclohexadiene rings. The nets in their paper differ from that shown in **2**, in which there are no sp³—sp³ carbon bonds.

symmetry, and a ratio of "trigonal" to "tetrahedral" atoms of 2:1, consistent with the 1,4-cyclohexadiene building block.


2
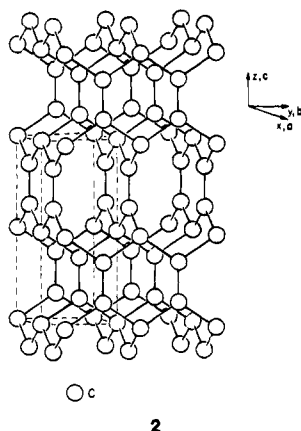
Assuming, after the previously determined 1,4-cyclohexadiene structure,[6] carbon—carbon single bond lengths of 1.51 Å, carbon—carbon double bond lengths of 1.35 Å, a trigonal bond angle of 123°, and a tetrahedral bond angle of 114°, the calculated density of **2** is 3.12 g/cm³, intermediate between graphite (2.27 g/cm³) and diamond (3.55 g/cm³).

The lattice is composed of ethylenic columns which run along the **a** (*x*) and the **b** (*y*) directions in the tetragonal structure. From another perspective, the lattice can be viewed as containing chains of alternating trigonal and tetrahedral carbons running at right angles to each other from the basal plane along the **c** axis. Seen in this way, this tetragonal structure is then the middle member of a sequence of related structures. In diamond (space group $F4_1/d3m$, No. 227) polyethylene chains run at right angles to each other from a plane of the cubic unit cell along an edge. In a hypothetical metallic allotrope of carbon (space group $I4_1/amd$, No. 141) described earlier[7] and based upon the Si network in the ThSi₂ structure, polyacetylene chains run at right angles to each other from the basal plane along the **c** axis in the unit cell.

It is useful to approach the bonding in this net by examining several substructures in it. These make it easier both to visualize the net and to point to the chemically significant units in it. Such substructures will also serve as one- and two-dimensional models for the electronic structure of the full lattice.

The first such one-dimensional substructure in the net, one that incorporates the 1,4-cyclohexadiene rings, is **3**, which we will call the "polyquinoid" substructure. When it comes to


3
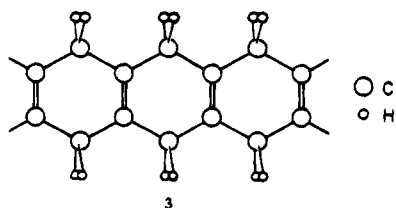
carrying out a calculation on a given substructure, we need to "terminate" it where it is cut from the three-dimensional net. This is accomplished simply in this case by adding 2 H's to the open valences on the tetrahedral carbon atoms, as shown in **3**.

(6) (a) Carreira, L. A.; Carter, R. O.; Durig, J. R. *J. Chem. Phys.* **1973**, *59*, 812. (b) Oberhammer, H.; Bauer, S. H. *J. Am. Chem. Soc.* **1969**, *91*, 10. The structural information is based upon electron diffraction data of the gaseous 1,4-cyclohexadiene molecule. Carreira et al. report the ring in a planar equilibrium conformation.

(7) Hoffmann, R.; Hughbanks, T.; Kertesz, M.; Bird, P. H. *J. Am. Chem. Soc.* **1983**, *105*, 4831.

Another one-dimensional substructure of **2** is obtained by focusing on the 1,4-cyclohexadiene rings linked through the tetrahedral carbon atoms. This is the "polyspiroquinoid" substructure, shown in **4**. Once again, a realistic one-


4
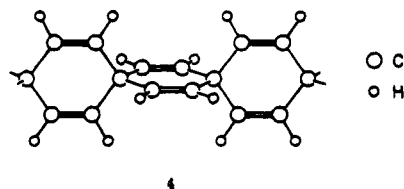
dimensional polymer model is formed by adding 6 H's per unit cell to satisfy the valence requirement of carbon.

A third one-dimensional substructure to be seen in **2** is that of the stacked olefins. A model may be constructed by linking the 1,4-cyclohexadiene rings through bridging methylene groups. We will call this the "polycyclophane" substructure, shown in **5**. A fully bonded model adds 8 H's per unit cell of 8 carbons to satisfy the valence requirement of carbon.


5
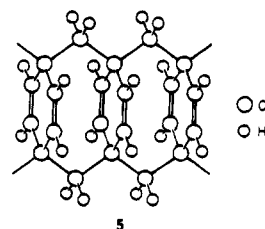
As we will see, each of the one-dimensional models will bring out a certain electronic feature of the full lattice. On the way to the three-dimensional structure we will also look at a two-dimensional layer. By joining polyspiroquinoid chains through edge-sharing of the three-connected vertices the two-dimensional "spriographite" substructure of the tetragonal lattice is obtained, as shown in **6**.

6
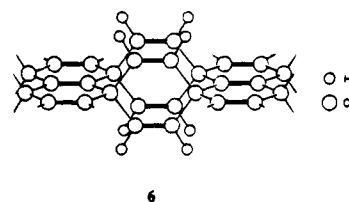
One final preliminary note: the full three-dimensional structure of this tetragonal carbon[8] is related to that of cooperite, PtS, shown in **7**. To move from one structure to the other, one replaces square planar platinum vertices with carbon atom pairs and changes the tetrahedral sulfur atoms into carbon atoms.

7
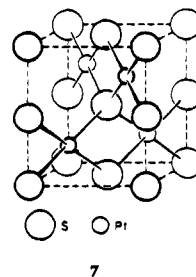
(8) The name glitter is suggested for the tetragonal carbon phase described in this paper owing to its semi-metallic electronic structure. Cf. "All that glitters is not gold..." W. Shakespeare, Merchant of Venice, Act II, Sc. 7, 1665.
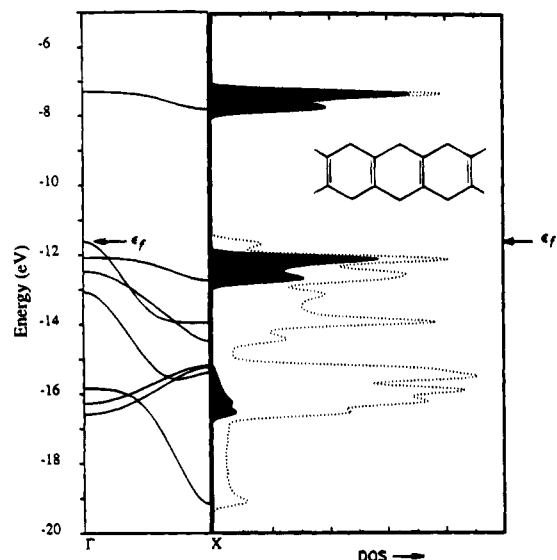
Figure 1. Band structure, on the left, and density of states profile, on the right, for the one-dimensional polyquinoid structure, model **3**. The contribution from the π-bonded p-orbitals is shown as the shaded area in the DOS profile.

Figure 2. Band structure, on the left, and density of states profile, on the right, for the one-dimensional polyspiroquinoid structure, model **4**. The contribution from the π-bonded p-orbitals is shown as the shaded area in the DOS profile.
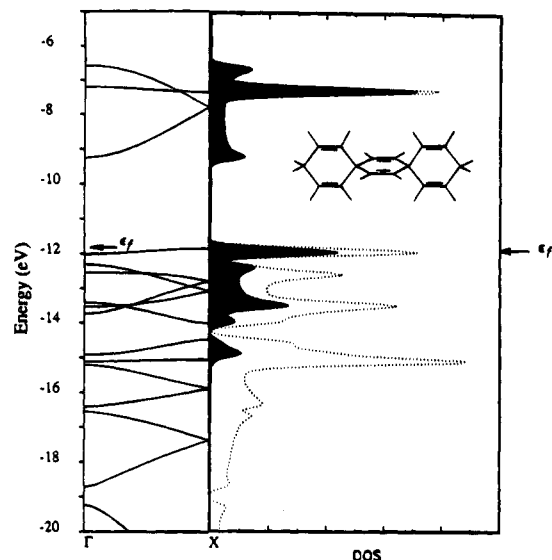
Electronic Structure of Models

The full 3,4-connected net and all the one- and two-dimensional models carved out of it contain unconjugated double bonds. Were those double bonds far apart in space, we would expect a substantial gap between filled and unfilled levels (or bands). However, the geometric constraints of the structure (see **5** or **6**) force unconjugated double bonds face-to-face onto each other. The separation between those π systems is 2.53 Å in our models. A normal van der Waals π contact is approximately 3.3 Å, the interlayer spacing in graphite. At the shorter 2.53 Å contact there will be a substantial broadening of the π and π* bands,[4] and a consequent narrowing of the gap between them. There is the potential of the closing of that gap, so that a conducting system is achieved. Let us examine the various low-dimensional models with these considerations in mind.

In polyquinoid, **3**, and polysprioquinoid, **4**, the π-bonded carbon atom pairs are oriented so that the π bonds are parallel to (in different ways in each structure) and far away from each other. As reflected in their density of states (DOS) profiles, these should be and indeed turn out to be wide band-gap one-dimensional substructures of the full tetragonal carbon lattice described here.

Figure 1 shows the band structure of polyquinoid, **3**, and its corresponding density of states (DOS).[9] The π-bonding p-orbital contribution of the total density of states is also shown. It is clear from this projection that the π-bonding p-orbitals contribute to the DOS at 1 eV below the Fermi level and to the empty states immediately across the band gap in polyquinoid. Interestingly, the states just below the Fermi level are involved in the tetrahedral-to-trigonal carbon σ bonding. The narrowness of the π-type bands testifies to the lack of through-space interaction in these polyolefins.

The band structure and DOS of the polyspiroquinoid model **4** are shown in Figure 2. The indicated projection of the total DOS shows that the states near and at the Fermi level (−11.87 eV) are largely composed of π-bonding p-orbitals. Note in Figure 2, the band structure diagram, that these bands are

somewhat wider than in polyquinoid. The gap is narrowed but not closed.

There is a curious detail in the electronic structure of this model which makes a connection to spiroconjugation, a bonding concept introduced some years ago by one of us, and simultaneously by Simmons and Fukunaga.[10] Consider a formally unconjugated system in which a spiro carbon atom is flanked by four π systems, here symbolized by single p-type orbitals, **8**.
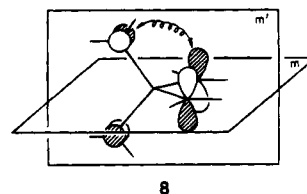
The four π systems (containing π or π* orbitals) generate various symmetry-adapted combinations of SS, SA, AS, and AA symmetry (S = symmetric, A = antisymmetric, first with respect to one plane, m, then with respect to the other, m').

Of these combinations, the AA is unique in allowing, to the extent there is a through-space overlap, interaction between the π systems. The AA combination is shown in **8**. The coupling overlap (shown by a squiggly line in **8**, there are four such) is small, 0.00549 in the geometry of the polyspiroquinoid model. For comparison, direct π overlap between the p orbitals in an ethylene double bond is 0.274. Nevertheless, the overlap across the spiro carbon is sufficient to produce a noticeable effect, the opening up of a gap between the bonding and the antibonding AA combinations. There are some observable consequences of this kind of conjugation.[11]

In the polyspiroquinoid model **4**, the spiroconjugation manifests itself in a greater dispersion of the π* band (compare Figure 1 to Figure 2). But spiroconjugation is insufficient to reduce the band gap significantly.

With the polycyclophane one-dimensional polymer, **5**, we approach a model that is more likely to capture the essential

(9) Hoffmann, R. *Solids and Surfaces: A Chemist's View of Bonding in Extended Structures*; VCH Publishers: New York, 1988.

(10) (a) Hoffmann, R. H.; Imamura, A.; Zeiss, G. *J. Am. Chem. Soc.* **1967**, *89*, 5215–5220. (b) Simmons, H. E.; Fukunaga, T. *J. Am. Chem. Soc.* **1967**, *89*, 5208–5215.
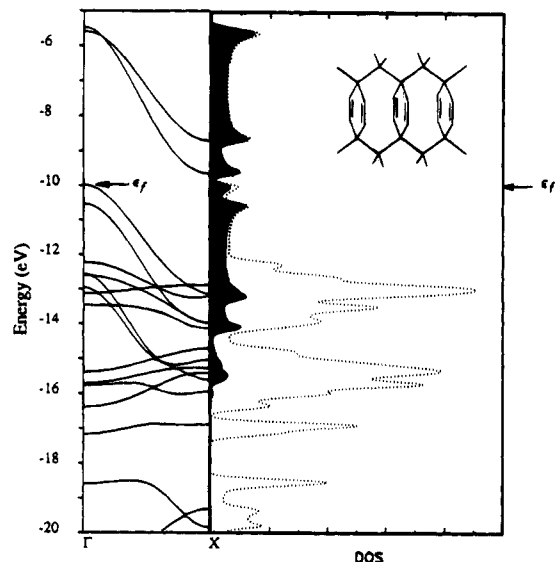
Figure 3. Band structure, on the left, and density of states profile, on the right, for the one-dimensional polycyclophane structure, model **5**. The contribution from the π-bonded p-orbitals is shown as the shaded area in the DOS profile.
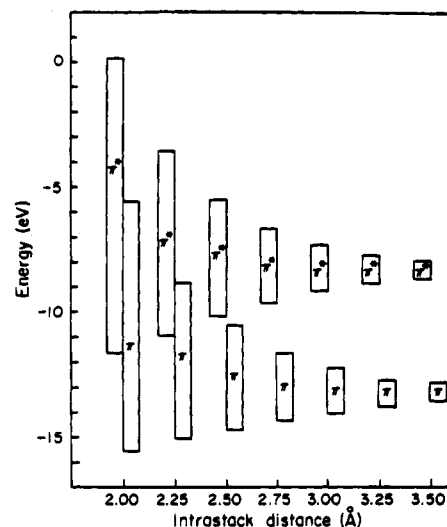
features of the three-dimensional 3,4-connected net. In **5** we have the important through-space overlap of the olefins. Indeed in the band structure of **5**, shown in Figure 3, we see wide π and π^* bands. These π-type bands, the highest filled and the lowest unfilled bands at the zone center in the band diagram, come in pairs (two π and two π^* levels per unit cell) that "run down" to the zone edge.[4]

The substantial dispersion of the π and the π^* states (see Figure 3 right for a demonstration that these bands are composed of olefinic p_π-orbitals) produces a very small band gap. This is the first indication of where band overlap at the Fermi level will occur in the three-dimensional hypothetical carbon structure.

The high π- and π^*-band dispersion in the polycyclophane substructure is a consequence of the small separation between the π-bonded carbon pairs that are interacting through space. A relevant model here is **9**, a column of ethylenes. In that array, as the inter-ethylene separation, **a**, decreases, the π and π^* bandwidths increase,[4] as shown in Figure 4.

9
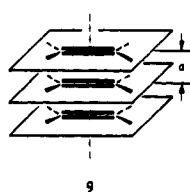
Below approximately 2.5 Å, the through-space interaction of an ethylene column leads to π- and π^*-band overlap.[4] The 3,4-connected net we are studying and the models derived from it, such as **5**, have an ethylene—ethylene separation of 2.53 Å, just approaching that crossing point. At 2.53 Å, the σ overlap of

(11) (a) Galasso, V. *Chem. Phys.* **1991**, *153*, 13—23. (b) Smolinski, S.; Balazy, M.; Iwamura, H.; Sugawara, T.; Kawada, Y.; Iwamura, M. *Bull. Chem. Soc. Jpn.* **1982**, *55*, 1106—1111. (c) Simkin, B. Y.; Makarov, S. P.; Furmanova, N. G.; Karaev, K. S.; Minkin, V. I. *Chem. Heterocycl. Compd.* **1978**, 948—959. (d) Durr, H.; Gleiter, R. *Angew. Chem., Int. Ed. Engl.* **1978**, 17, 559. (e) Batich, C.; Heilbronner, E.; Rommel, E.; Semmelhack, M. F.; Foos, J. S. *J. Am. Chem. Soc.* **1974**, *96*, 7662—7668. (f) Sustmann, R.; Schubert, R. *Angew. Chem., Int. Ed. Engl.* **1972**, *11*, 840. (g) Garbisch, E. W., Jr.; Sprecher, R. F. *J. Am. Chem. Soc.* **1966**, *88*, 3433, 3434. (h) Eaton, P. E.; Hudson, R. A. *J. Am. Chem. Soc.* **1965**, *87*, 2769. (i) Houk, K. N. *J. Am. Chem. Soc.* **1965**, *87*, 2769.


Figure 4. The effect of the intrastack separation, *a*, in an ethylene stack on the dispersion of its π and π^* bands. Note that at about 2.5 Å $\pi-\pi^*$ band overlap begins.
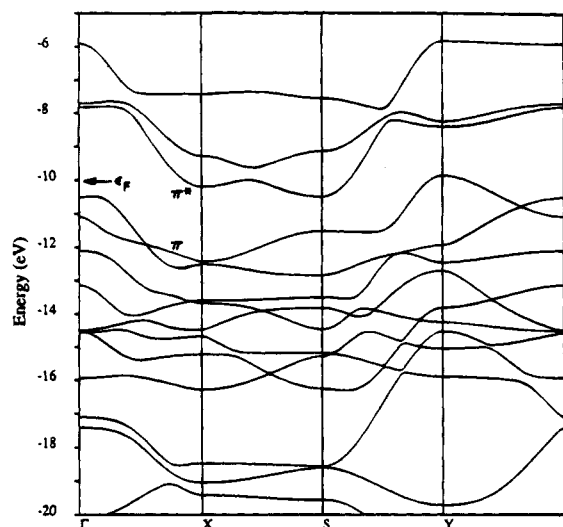
Figure 5. Band structure of the two-dimensional spirographite structure, model **6**. The π and π^* bands run in pairs down from the zone center Γ to symmetry point X in the Brillouin zone. This is reminiscent of the band structure in polycyclophane.
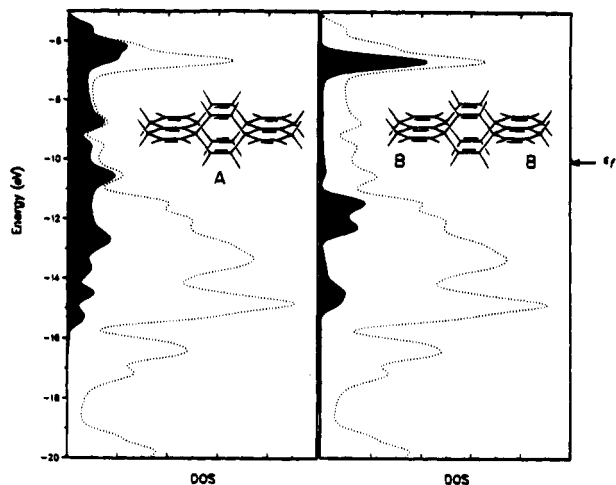
two 2p orbitals of neighboring olefins, **10**, is 0.120, sufficient to produce substantial dispersion.
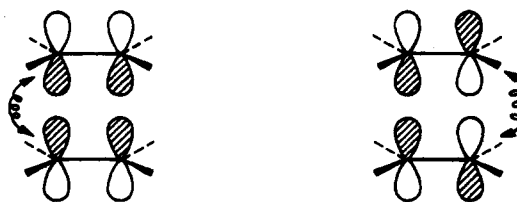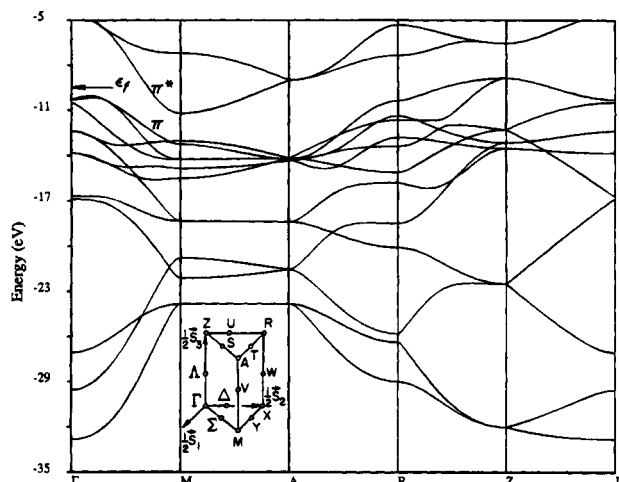

10

Spirographite, **6**, has two types of π-bonded carbon atoms in its structure. Some double bonds are stacked, with strong through-space interactions, while others are in a polyquinoid chain. In the band diagram shown in Figure 5, one can see that traveling along the symmetry line from Γ to X in the Brillouin zone, the π and π^* bands are quite dispersed. This is the reciprocal space direction corresponding to the stacking axis of the ethylene column in real space. The resemblance of this section to the polycyclophane band structure is clear. Note the

Figure 6. Density of states profiles of spirographite structure, model 6. The left panel shows the projection of the through-space interacting π-bonded p-orbitals in the shaded area (stack A) while the right panel shows the projection from the π-bonded p-orbitals in the polyquinoid chain in the shaded area (stack B). Note the contribution to the DOS across the Fermi level of the through-space interacting p-orbitals in spirographite.
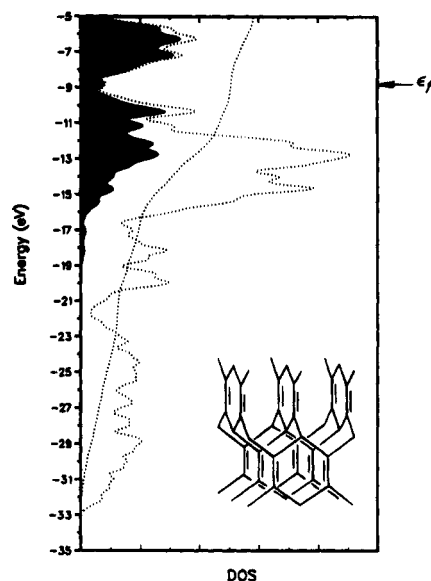

Figure 8. Density of states profile of tetragonal carbon, net **2**, with projection of the π-bonded p-orbitals indicated. Note that these orbitals contribute nearly exclusively to the DOS about the Fermi level in this tetragonal carbon structure.

Figure 7. Band structure of tetragonal carbon, **2**. Note that in the energy window shown from −35 to −5 eV, there are 14 bands shown out of a total of 24. There are two π and two π* bands in the unit cell. These are the highest filled (two π bands) and lowest unfilled (two π* bands) bands in the structure.

small band overlap in this structure, the first time in this series of models that we encounter a potential conducting system.

We can dissect the contributions of the polycyclophane and polyquinoid units to the electronic structure of this two-dimensional net. Figure 6 shows that the states near the Fermi level are predominantly derived from the stacked olefin one-dimensional substructure contained in spirographite. In contrast, states from the polyquinoid substructure do not occur near the Fermi level.

The Three-Dimensional 3,4-Connected Carbon Net

The full three-dimensional tetragonal carbon material drawn in **2** contains ethylenes stacked at a separation of 2.53 Å. The ethylene columns run perpendicular to each other to generate the full three-dimensional structure. The models we examined so far were cut out of the full net, **2**, and we expect to see features of all of them in the electronic structure of **2**. The band structure of **2** is shown in Figure 7.

Important for considerations of conductivity is the potential overlap of the highest filled and lowest unfilled bands in this tetragonal structure of carbon. Inspection of the band diagram for this structure (Figure 7) reveals that there is a significant degree of indirect band overlap across the Fermi level. Along the symmetry line Γ to M, and then along the symmetry line from R to Z (in the Brillouin zone of tetragonal carbon), the highest filled, π-band is near its highest energy point; while at symmetry point M, the lowest unfilled band, the π*-band, is at its lowest energy point. It is evident that these bands have an indirect overlap.

The DOS profile in Figure 8 reflects this band overlap, showing a density of states at the Fermi level (−9.62 eV). Because the actual overlap is substantial, there is a DOS at the Fermi level. Note that the main contribution to the DOS for several electronvolts below and above the Fermi level is provided by the π-bonding p-orbitals of the trigonal carbons. The energy window shown in Figure 8 is wider than in our earlier discussion of the models, so as to facilitate forthcoming comparisons with other nets.

The crystal orbital overlap population (COOP) plots[9] for the tetrahedral-to-trigonal carbon bond and the trigonal-to-trigonal carbon bond are shown in Figure 9. COOP curves are indicators of the bonding capability of the orbitals at a given energy.

For the tetrahedral-to-trigonal carbon bond, the COOP curve shows that there is a bonding interaction all the way up to the Fermi level. In the case of the trigonal-to-trigonal carbon bond, the crossover from bonding to antibonding states nearly coincides with the Fermi energy, but is actually bonding up to this point (−9.62 eV). The overlap population for the tetrahedral-to-trigonal carbon bond is 0.795, while the overlap population for the trigonal-to-trigonal carbon bond is 1.324. All this is consistent with the chemically intuitive single and double bonding in the structure.

We computed a total energy for the tetragonal carbon net, with unit cell dimensions of a = 2.53 Å and c = 5.98 Å. These dimensions are based upon a 1,4-cyclohexadiene model molecule;[6] the geometrical parameters were specified in the introduction. The total energy is −70.14 eV/C atom, compared to −70.26 eV/C atom for the hypothetical metallic allotrope of carbon reported previously[7] and −71.00 eV/C atom for hex-

3,4-Connected Carbon Net from Cyclohexadiene Rings

J. Am. Chem. Soc., Vol. 116, No. 25, 1994 11461
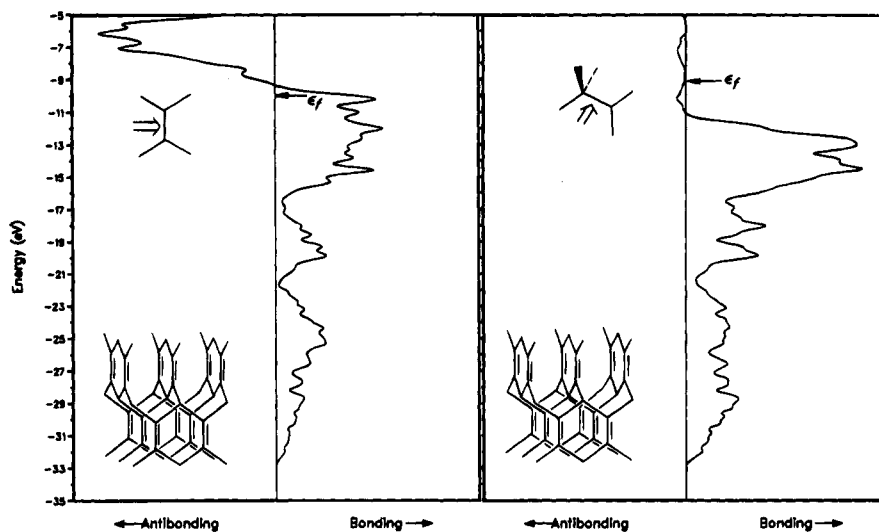
Figure 9. COOP curves for tetrahedral-to-trigonal carbon (right) and trigonal-to-trigonal carbon bonds (left). Crossover from bonding to antibonding occurs at the Fermi level for trigonal-to-trigonal bonding in this tetragonal carbon structure.

agonal graphite. The extended Hückel method is not reliable for energetics, especially when different coordination numbers are involved. Nevertheless, it is clear that the 3,4-connected net is thermodynamically quite unstable. If made, however, it should persist, for the barriers to rearrangement to graphite or diamond are likely to be large.

Aside from its possible conductivity, yet another interesting feature of this 3,4-connected material, as a result of the short interatomic distances it has, is the high bulk modulus predicted for it based upon Cohen's semiempirical formula.[12]

$$B_0 = (1972 - 220I)d^{-3.5}\langle N_c \rangle/4 \text{ GPa} \qquad (1)$$

Here $\langle N_c \rangle$ is the weighted average coordination number, which is $3^{1/3}$ in the 3,4-connected net, I is the ionicity, which is 0 for the all-carbon material, and d is the weighted average bond distance in the covalently bonded material, which is 1.46 Å for tetragonal carbon. The formula is dimensionally correct for bond lengths in angströms to yield bulk moduli in gigapascals (10 kbar = 1 GPa). At a calculated value of 440 GPa, the bulk modulus of this tetragonal structure of carbon is 1.14% (5 GPa) higher than the bulk modulus of diamond calculated from the Cohen semiempirical theory (435 GPa, experimental 442 GPa[13]). Since the bulk modulus scales as $d^{-3.5}$, the high value of **2** is simply a consequence of the relatively short bonds in the structure.[14]

3,4-Connected B₂C and CN₂ Nets

Three-connection is a typical coordination pattern for boron and nitrogen, so it makes sense to consider derivatives of **2** based upon replacement of the trigonal carbon atoms in **2** with boron atoms and, alternatively, with nitrogen atoms.[15] These three hypothetical phases patterned on the $P4_2/mmc$ space group form

(12) Cohen, M. L. *Phys. Rev. B* **1985**, *32*, 7988.

(13) McSkimin, H.; Andreatch, P. *J. Appl. Phys.* **1972**, *43*, 2944.

(14) (a) Ruoff, R. S.; Ruoff, A. L. *Nature* **1991**, *350*, 663. (b) Ruoff, R. S.; Ruoff, A. L. *Appl. Phys. Lett.* **1991**, *59*, 1553. Ruoff and Ruoff present an interesting analysis of the fullerite bulk modulus. By applying a simple mechanical model treating the fullerene molecules as hard spheres, with their icosahedral symmetry and the C—C bond strength, they estimated the bulk modulus for fullerite at pressures above 20 GPa. The computed bulk moduli are considerably higher (620—670 GPa) than those of diamond or β-C₃N₄.

(15) In Appendix 2 we provide the theoretical diffraction pattern of **2** and of the B and N substituted lattices for a diffraction experiment with Cu Kα radiation.
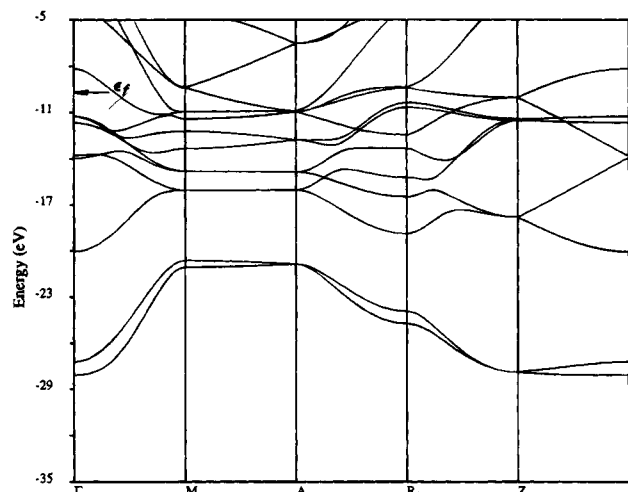
Figure 10. Band structure of tetragonal B₂C. In the energy window from −35 to −5 eV the 12 lowest bands are completely shown, with bands 13 and 14 partially shown. Touching of the highest occupied band (the tenth band) and the lowest unoccupied band (the eleventh band) occurs near symmetry point M in the Brillouin zone and they are degenerate along the symmetry line from M to A.

an interesting sequence. As we will see below, in the CN₂ phase there is a wide band gap between the highest occupied and lowest unoccupied bands. In contrast, there is substantial direct band overlap in the B₂C phase.

With borons occupying the trigonal sites in B₂C, a theoretical density of 2.44 g/cm³ is calculated based upon a B—B bond length of 1.72 Å[16] and a C—B bond length of 1.56 Å,[17] with the B—B—C bond angle set at 123° and the "tetrahedral" carbon bond angle set at 114°. In comparison, the rhombohedral B₄C phase,[18] a known boron—carbide phase, has a density of 2.52 g/cm³.

The band diagram for the tetragonal B₂C structure is shown in Figure 10. Like the carbon structure, it has 24 bands, only

(16) Danielson, D. D.; Patton, J. V.; Hedberg, K. *J. Am. Chem. Soc.* **1977**, *99*, 6484. Structural information for the B—B bond was obtained from electron diffraction of gaseous B₂F₄.

(17) Langridge-Smith, P.; Stevens, R.; Cox, A. *J. Chem. Soc., Faraday Trans.* **1979**, *75*, 1620.

(18) (a) Ridgeway, R. R. *Trans. Electrochem. Soc.* **1934**, *66*, 117—133. (b) *Boron-Rich Solids*; Emin, D., Aselage, T., Switendick, A. C., Morosin, B., Beckel, C. L., Eds.; A.I.P. Conference Proceedings 231, Albuquerque, New Mexico, 1990; American Institute of Physics: New York, 1991.
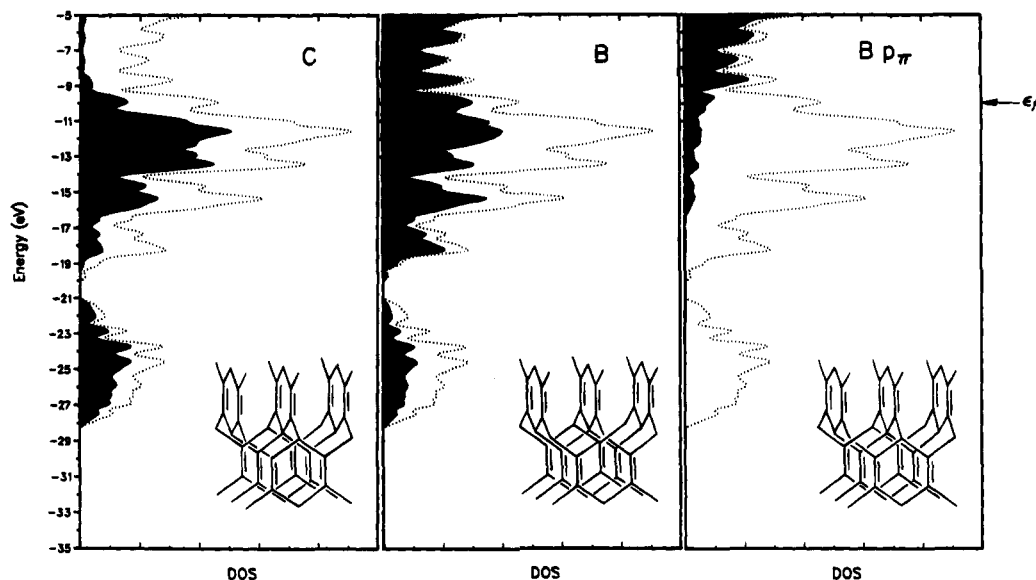
Figure 11. Density of states profile of B_2C, with projection of the carbon (left) and boron (middle) contributions to the DOS shown in the shaded areas. Note that the orbitals on the trigonal boron atoms contribute nearly exclusively to the DOS about the Fermi level in this tetragonal structure. In the right panel is shown the projection of the π-bonding p-orbitals of the boron atoms in the unit cell in the shaded area. There is a small contribution of states derived from these orbitals at the Fermi energy.
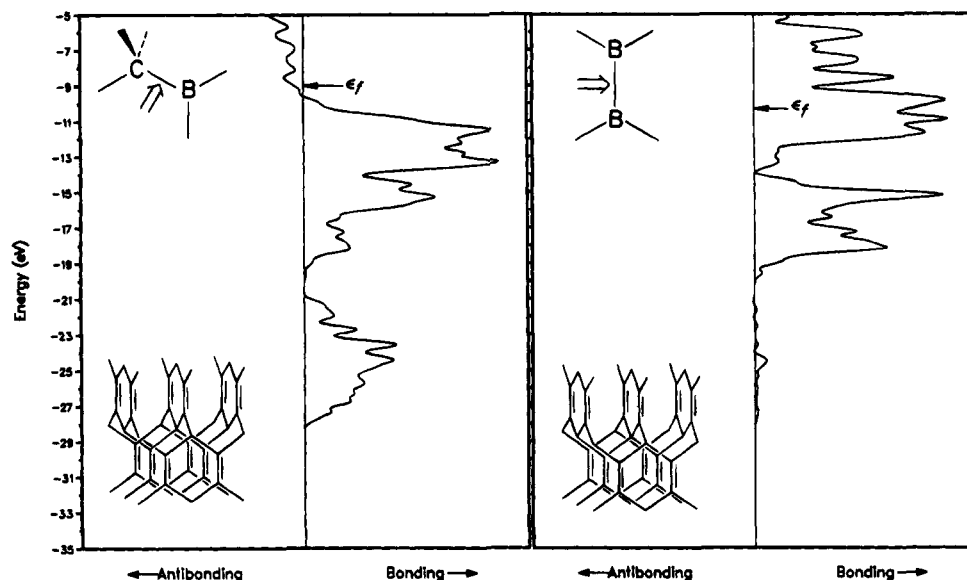
Figure 12. Crystal orbital overlap population curves for carbon-to-boron bonding (left) and boron-to-boron bonding (right) in B_2C. Note the strongly bonding profile for the boron−boron interaction up to and well above the Fermi level. The carbon−boron interaction has a slight antibonding component just below the Fermi level.

12 of which are shown. Of these bands, the 20 valence electrons in the B_2C unit cell fill the lowest 10 bands of the phase. The band structure of B_2C (Figure 10) is qualitatively similar to that of the parent pure carbon net (Figure 7). This is not surprising, since most of the features of the band structure are determined by the symmetry of the lattice.

As shown in Figure 10, there is substantial direct band overlap at the Fermi level in the B_2C structure; this suggests that phase would be metallic. From a projection of the boron and the carbon contributions to the DOS (Figure 11) it is clear that states about the Fermi level are largely derived from boron. A few of the B π-bonding p-orbital states are filled, as can be seen in the third projection in Figure 11, but mostly these are empty. The actual population of a B $2p_\pi$-orbital (one perpendicular to the trigonal B plane) is 0.121.

Shown in Figure 12 are the crystal orbital overlap populations for the B_2C structure. The average overlap population is 0.795

for the carbon−boron bond. The B−B COOP shows there is substantial bonding at and above the Fermi level for the boron− boron bond. The B−B overlap population in B_2C is 0.871. B−B π-bonding states are only slightly filled. An adjacent B−B $p_\pi-p_\pi$ overlap population is calculated to be 0.0300 in our model B_2C structure; we have a B−B single bond, not a double bond.

Nitrogen atoms can be placed in the trigonal sites to generate the CN_2 structure. Of course, N wants to be pyramidal and not trigonal, so such a structure is not expected to be very stable. The theoretical density, 3.61 g/cm³, is calculated based on an N−N bond length if 1.45 Å[19] and a C−N bond length of 1.47

(19) Kohata, K.; Fukuyama, T.; Kuchitsu, K. *J. Phys. Chem.* **1982**, *86*, 602. Hydrazine was studied in the gas phase by electron diffraction. Electron diffraction intensity data together with the rotational constants for hydrazine previously reported by Kasuya (*Sci. Pap. Inst. Phys. Chem. Res.* **1962**, *56*, 1) were used to determine the structure of the molecule.
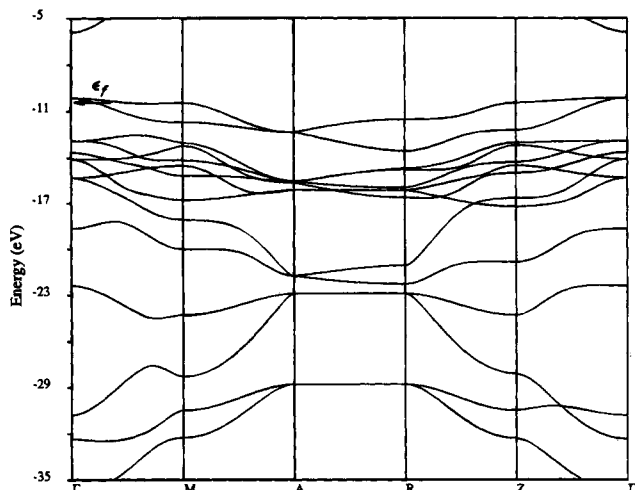
Figure 13. Band structure of tetragonal CN_2. In the energy window from -35 to -5 eV the 14 lowest bands are completely shown, with band 15 partially shown. There is a substantial gap (3−4 eV) between the highest occupied band (14) and the lowest unoccupied band (15) in the band structure of CN_2.

Figure 14. Density of states profile of CN_2, with projection of the carbon (left) and nitrogen (right) contributions to the DOS as the shaded areas. This diagram shows the substantial gap in states above the Fermi level and indicates this phase to be an insulator.

Å,[20] with the N−N−C bond angle set at 123° and the "tetrahedral" carbon bond angle set at 114°. Recently there was reported the synthesis of a β-C_3N_4 phase,[21] patterned on the β-Si_3N_4 structure. Although electron diffraction of the material clearly showed lines that could be indexed to a hypothetical β-C_3N_4 structure, no experimental density was reported. The electronic structure of C_3N_4 has been studied as well.[22]

The band diagram for the CN_2 structure is shown in Figure 13. Like the other structures patterned on **2**, it has 24 bands (only 14 bands are shown). Of these bands, 14 are filled, since there are 28 valence electrons in the unit cell of the CN_2 phase. As can be seen in the band diagram, there is a substantial gap between the fourteenth band, the highest occupied band, and the fifteenth band, the lowest unoccupied band. That energy separation is at least 4 eV; the CN_2 phase would be a wide band gap insulator. The DOS (Figure 14) confirms this, it also indicates the states right below the Fermi level are mainly nitrogen in character. A COOP curve (not shown here) indicates these states are N−N antibonding. As a result the N−N overlap population is relativley low, 0.566. There is evidence in the electronic structure of N−N repulsion.

The Band Gap and the Trigonal Atom Electron Count

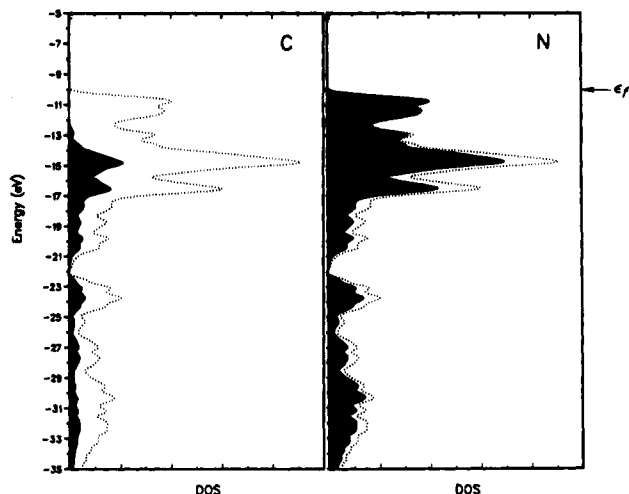Why is there such a dramatic difference in the electronic structure as one moves along the sequence from B_2C to tetragonal carbon to CN_2? The band structures are similar, but the electron count is different. And this clearly affects the bonding.

The easiest way to see what is happening is to think of the B_2 or N_2 unit of B_2C or CN_2 is isoelectronic with C_2^{2+} and C_2^{2-}, respectively. The states around the Fermi level are derived from the p_π-orbitals of the trigonal centers, so let us consider the ethylene model of **11**. The relevant molecules are $C_2H_4^{2+}$,

C_2H_4, and $C_2H_4^{2-}$, each trigonal. The actual geometries of the cations and the anions will differ.[23]

11

It is clear that in ethylene (or the tetragonal carbon structure, **2**) there is a π level filled, i.e. maximal π bonding. In $C_2H_4^{2+}$ or B_2H_4 that level is empty. There is no net π bonding. In $C_2H_4^{2-}$ or N_2H_4 the π^* orbital is occupied; again there is no net π bonding, as both π and π^* levels are filled. Instead there will be lone pair−lone pair repulsion. Of course, isolated hydrazine would twist and pyramidalize to minimize lone pair repulsion.[24] It cannot do so in the present three-dimensional net.

This simple picture explains the diminished B−B and N−N bonding, but not the conductivity computed for the tetragonal carbon material and for B_2C. In the latter, the higher lying B−B and B−C σ bands overlap with the bottom of the π band. Thus even though one might not have expected a structure with B−C and B−B single bonds to be conducting, this hypothetical one is.

The tetragonal carbon net discussed here represents an electronically interesting, dense structure that from the point of view of carbon coordination is intermediate between diamond and graphite. Structurally it is very different from the other carbon allotropes. It would be fun if it could be made.

(20) Oberhammer, H.; Günther, H.; Bürger, H.; Heyder, F.; Pawelke, G. *J. Phys. Chem.* **1982**, *86*, 664. CF_3NF_2 was studied in the gas phase by electron diffraction and by microwave spectroscopy. From analysis of both sets of data the molecular structure of perfluoromethylamine was determined.
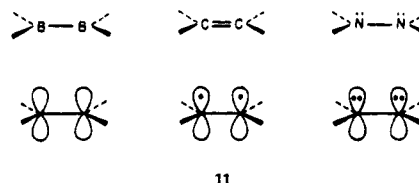
(21) Niu, C.; Lu, Y.; Lieber, C. M. *Science* **1993**, *261*, 334. Thin films of β-C_3N_4 were deposited onto a Si(100) or polycrystalline Ni surface through reaction of laser ablated carbon vapor with an atomic nitrogen beam directed at the substrate surface.

(22) Hughbanks, T.; Tian, Y., to be submitted for publication.

(23) (a) Hollenstein, S.; Laube, T. *J. Am. Chem. Soc.* **1993**, *115*, 7240–7245. (b) Graul, S. T.; Squires, R. R. *J. Am. Chem. Soc.* **1990**, *112*, 2506–2516. (c) March, J. *Advanced Organic Chemistry*; Wiley: New York, 1985. Structures of the $C_2H_4^{2+}$ and B_2H_4 molecules, and the $C_2H_4^{2-}$ and N_2H_4 molecules, were obtained with a full geometry optimization using the Hartree−Fock method with the STO-3G basis set. The calculations were run using the Spartan computational chemistry code provided to us by Warren Hehre of Wavefunction, Inc. In the former case the empty p_π-orbital leads to a planar geometry for these molecules. In the latter case the filled p_π-orbital leads to pyramidalization about the trigonal atom with the lone pairs trans to each other. Both of these molecular calculations are in agreement with chemical intuition based upon the valence shell electron pair model.

(24) Pannetier, A. *Bull. Soc. Chim. Fr.* **1972**, 2623.

(25) Anderson, A. B.; Hoffmann, R. *J. Chem. Phys.* **1974**, *60*, 4271.

Appendix 1

Parameters used in the calculations described in this paper, summarized in Table 1, are taken from the literature: H,[25] B,[26a] C,[26a] and N.[26a] The extended Hückel method is already well documented[26] so that its description here is not necessary. The adaptation of the extended Hückel method to extended structures

Table 1. Atomic Parameters Used in the Calculations

element	orbital	H_{ii} (eV)	ζ(STO)
H	1s	−13.6	1.300
B	2s	−15.2	1.300
B	2p	−8.5	1.300
C	2s	−21.4	1.625
C	2p	−11.5	1.625
N	2s	−26.0	1.950
N	2p	−13.4	1.950

is described in ref 9 and the references therein. Symmetry lines followed in the band calculations are based upon the specifications in the paper by Ramirez and Böhm[27] on the use of symmetry in reciprocal space integrations.

Appendix 2

Theoretical diffraction patterns are calculated for each of the tetragonal structures described in the paper and are given in Table 2 in the supplementary material to this paper.[28] They may be of use to experimental investigators of new carbon phases. Tables 2a, 2b, and 2c list the calculated Bragg angles corresponding to the indicated d-spacings for a diffraction experiment using Cu Kα radiation at a wavelength of 1.5418 Å. The tables are for all reflections with $(h^2 + k^2 + l^2) \leq 12$. For space group No. 131, $P4_2/mmc$, the general reflection conditions are the following: hhl, $l = 2n$; 001, $l = 2n$.

(26) (a) Hoffmann, R. *J. Chem. Phys.* **1963**, *39*, 1397. (b) Hoffmann, R.; Lipscomb, W. N. *J. Chem. Phys.* **1962**, *37*, 2872.

(27) Ramirez, R.; Böhm, M. C. *Int. J. of Quant. Chem.* **1988**, *34*, 571.

(28) Supplementary material containing the diffraction patterns of the glitter lattices described in this paper can be obtained from the Department of Chemistry and Materials Science Center, Cornell University, Ithaca, New York 14853-1301, please address correspondence to Roald Hoffmann, John A. Newman Professor of Physical Science. The supplementary material consists of three separate pages.